International Journal for Applied Information Management
Vol. 3, No. 3, September 2023, pp. 118-124

Development of a Model for Recognizing Cracks on Concrete Surfaces Using Digital Image Processing Techniques

Yuzhong Kang[1,*] , Aimin Yu[1], Wenquan Zeng[1]

[1] Guangdong Vocational College of Science and Technology, College of Computer Science, Zhuhai, Guangdong, China, 519090
[1]kangyz19@zs.gdcxxy.net*
*corresponding author

(Received: June 22, 2023; Revised: July 5, 2023; Accepted: August 31, 2023; Available online: September 10, 2023)

Abstract

In this paper, the bridge crack detection method based on digital images is studied. In-depth analysis and evaluation are performed on the image processing algorithms such as image graying, resolution of checkerboard corner pixel rate, filtering denoising, and edge detection, etc. The calculation and software system for bridge crack width based on videos (or images) is implemented, and 15 bridge crack images are used to verify its crack detection accuracy. The results suggest that the proposed crack identification method in this paper can be used for the crack detection of reinforced concrete bridges and class B prestressed concrete bridges properly. When the crack width is greater than 0.3 mm, the calculated crack width value based on images is very close to the measured value.

Keywords: Concrete Bridge, Crack Detection, Digital Image, Computer Identification, Image Processing

1. Introduction

In daily inspections, routine examination of concrete bridges and the detection of cracks in the lower part of the beams play a pivotal role in ensuring structural integrity and safety of the bridge. Presently, the common approach involves deploying a lifting engineer to descend to the underside of the bridge beam, equipped with a simple crack detection device to measure crack width. Subsequently, this engineer manually records the crack's position, width, length, and other pertinent information [1-2]. However, this method exhibits several significant drawbacks.

Primarily, this manual approach has proven to be inefficient and time-consuming. The process of dispatching the lifting engineer, conducting manual observations, and meticulously documenting crack details consumes substantial time [3-4]. This not only impacts operational costs but also has the potential to disrupt traffic flow and bridge accessibility. Furthermore, this manual process tends to struggle in comprehensively grasping the widespread nature of crack occurrences and their attributes across the bridge surface. Cracks occurring in hard-to-reach or concealed areas can be easily overlooked.

Secondly, this manual approach is inadequate to meet the demands of modern bridge development. In an era where technology is rapidly advancing, a more sophisticated and automated approach is required to cater to the intricate and advanced requirements of modern bridges [5-7]. Contemporary bridges must not only meet higher safety standards but also operate efficiently and undergo continuous monitoring.

Within this context, there exists a significant research gap that warrants attention. Although several studies have proposed image-based crack detection methods, many of these focus predominantly on image processing with limited validation using real-field crack images [8-11]. Accurate validation of these methods is pivotal to ensuring reliable and precise outcomes in diverse field conditions.

Furthermore, it is imperative to acknowledge that research pertaining to crack detection and analysis in structural elements, particularly bridges, has undergone rapid development in recent years [12-13]. Numerous studies have proposed technology-driven image analysis approaches, such as employing image processing algorithms and

segmentation methods to identify cracks [14-15]. Nevertheless, there are technical challenges that need to be surmounted in order to achieve enhanced and more accurate results.

Some studies have employed image processing algorithms, including MATLAB, for crack segmentation on bridge surfaces [16-18]. Nevertheless, addressing local noise that may emerge in segmented images, such as pores, honeycombs, or surface peeling, remains an imperative. Some studies have also attempted pixel-based image cropping methods to calculate crack widths. Yet, the lack of emphasis on validation using actual crack images introduces uncertainties in measurement outcomes.

This paper aims to bridge this research gap by proposing a more comprehensive and validated approach to bridge crack detection [19]. Leveraging checkerboard calibration boards and more advanced image processing algorithms, this paper seeks to address image distortion issues, local noise challenges, and the consideration of real-field crack images. The anticipated outcome is a more substantial contribution to enhancing efficiency and precision in crack detection and measurement on bridges.

Within the context of bridge crack detection, there exists immense potential to amalgamate technological advancements in image analysis with practical field requirements. However, a holistic and integrated approach is essential to overcome the technical and operational constraints inherent in traditional methods. This paper strives to represent a forward step towards a deeper comprehension of bridge crack detection and offers a significant contribution to the development of safe and reliable infrastructure.

2. Bridge Crack Image Processing Techniques

2.1. Image Graying

This paper uses equation (1) to convert the RGB image into a grayscale image:

$$x = 0.30 \times R + 0.59 \times G + 0.11 \times B \quad (1)$$

Where x is the pixel rate value of the grayscale image; R, G, and B are the red, green, and blue component values of the pixel rate in the true-color image, respectively.

2.2. Gray Conversion

The grayscale conversion of crack images can improve the quality of the image and enhance the grayscale of the image [20]. The commonly used grayscale conversion methods are linear conversion and histogram conversion. This paper uses Equation (2) for linear conversion. The effect of image conversion is shown in Figure 1.

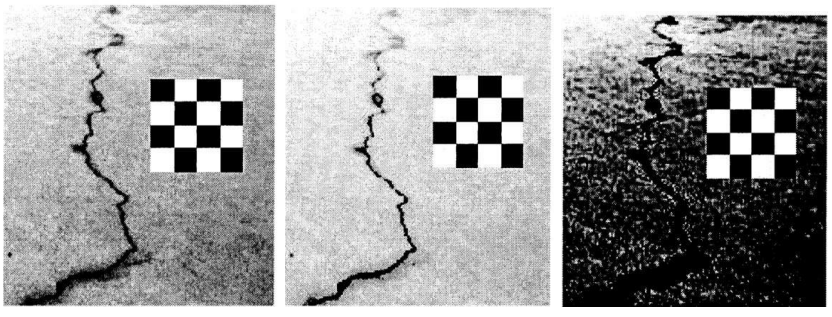

(a) Gray image conversion (b) Linear transformation (c) Histogram

Figure 1. Image conversion effects

$$g(x) = \{0, \frac{(x-T_{min})\times 255}{(T_{max}-T_{min})} 255, , \frac{\frac{x=T_{min}}{T_{min<x<T_{max}}}}{x=T_{max}} \quad (2)$$

Where g (x) is the converted grayscale pixel rate value; and are the minimum and maximum grayscale values in the image, respectively.

Figure 2 shows that the linear transformation better preserves the bridge crack details, further opening up the difference in gray values between the crack and the background, which is conducive to subsequent image processing and crack identification. Histogram conversion makes the gray distribution of the entire image more uniform. However, the gray value and crack width of the crack area in the image is deepened, which may cause a more significant error between the calculated crack width value and the actual value. Hence, linear grayscale conversion can better handle the bridge crack image.

2.3. Resolution of Image Pixel Rate

To meet the requirements of bridge crack identification, the checkerboard corner method is used to calculate the pixel rate of the image [21]. The image plane coordinate values of the checkerboard corner points (except the edge points) are calculated, and the pixel rate of the bridge crack image is calculated. The calculation equation is as follows: (3) shown:

$$\eta = \frac{D_1}{D_2} \tag{3}$$

Where η is the pixel rate (mm / pixel rate) of the image; D1 is the actual distance (mm) between the two corner points in the checkerboard; D2 is the pixel rate distance (pixel rates) between the two corner points in the checkerboard.
Currently, checkerboard corner detection can be divided into two types: straight line detection and corner detection. The straight line detection method first performs edge detection on the image, finds the straight line in the image, and finds the pixel rates of the checkerboard corner point by the intersection of the two straight lines. The coordinate corner detection method is based on the image gray detection method, which considers the gray value changes of pixel rates in the pixel rate area.

2.4. Image Filtering Denoising

Image filtering must effectively filter out noise in bridge crack images on the one hand, and effectively protect crack information on the other hand, and minimize blurring of crack edges during filtering to facilitate subsequent crack edge detection. This article uses actual bridge crack images as For the test object, several commonly used image filtering methods were systematically analyzed, and the average pixel rate deviation was used to evaluate the filtering effect of each algorithm.

1) Image Filtering Algorithm

Commonly used image filtering algorithms include smoothing filtering, median filtering, and mean filtering. In this paper, multiple bridge crack image filtering is used to improve the smoothing filtering, and a filtering method combining median and mean is studied.

The improved smoothing filter increases the gray value of a pixel rate point in a grayscale image to 4 times, the gray value of 4-pixel rates in adjacent top, bottom, left, and right to 2 times and the adjacent 4-pixel rates in the diagonal The gray value of the point is unchanged, then the gray values of 9-pixel rates are added and divided by 16 as the new gray value of the pixel rate.

The median and mean are filtered together, assuming that the gray value distribution of the pixel rates in the bridge crack image follows the normal distribution of F~N (μ, σ2). If the gray value of the image point is in [μ-2σ, μ+2σ], Mean filtering is used; if the gray value of the image point is outside [μ-2σ, μ+2σ], median filtering is used. The parameter μ, σ can be calculated using the gray value of the pixel rate:

$$\mu = \frac{1}{N}\sum_{i=1}^{N} x_i \tag{4}$$

$$\sigma\sqrt{\frac{1}{N}\sum_{i=1}^{N}(x_i - u)^2} \tag{5}$$

Where N is the total number of pixel rates in the bridge crack image; is the gray value of a pixel rate.

ISSN 2776-8007

2) Filtering Effect Evaluation

To evaluate the effect of various filtering algorithms on bridge crack images, the average pixel rate deviation evaluation method is adopted. Firstly, a noise with an average pixel rate deviation of 14.4957 is added to the original bridge crack grayscale image. Subsequently, different methods are used for filtering, and the filtering effects are shown in Figure 2.

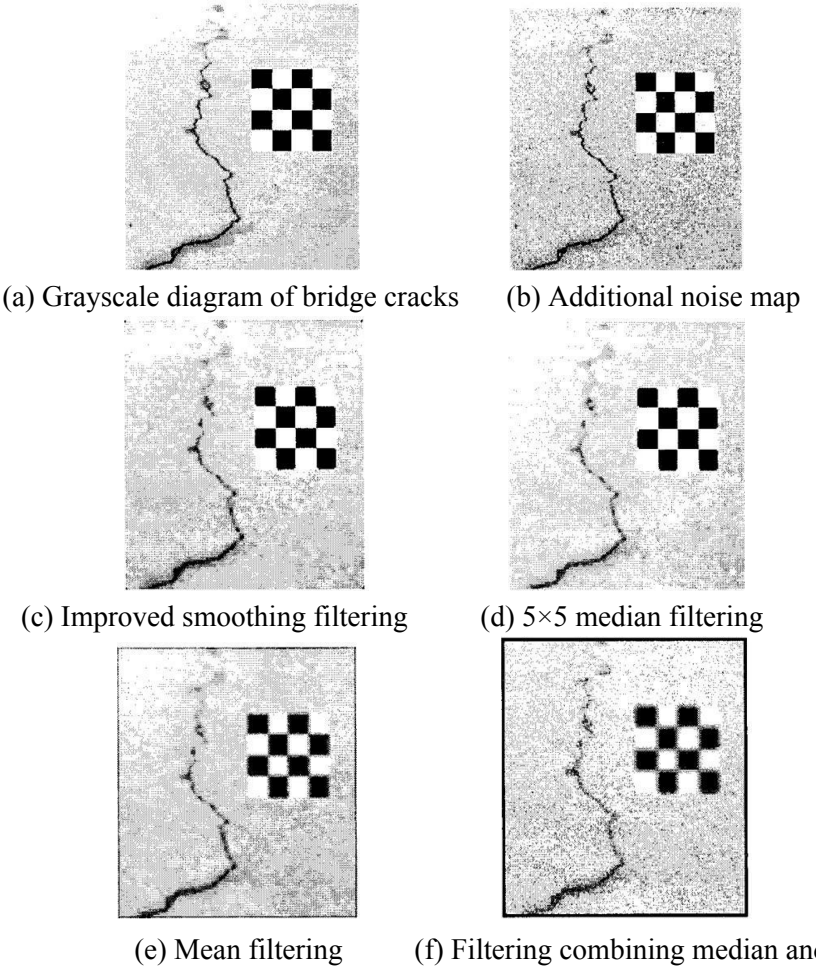

(a) Grayscale diagram of bridge cracks (b) Additional noise map

(c) Improved smoothing filtering (d) 5×5 median filtering

(e) Mean filtering (f) Filtering combining median and mean

Figure 2. Filtering effects of different algorithms

The filtered crack image is compared with the original grayscale image (that is, the grayscale image before noise is added). The smaller the average deviation of the grayscale value of the pixel rate, the better the filtering effect. The evaluation equation is as follows:

$$D\left(x_i\right) = \left|P\left(x_i\right) - M(x_i)\right| \tag{6}$$

$$A = \sum_{i=1}^{N} D(x_i)/N \tag{7}$$

Where P(xi) is the gray value of a pixel rate in the original gray map of the bridge crack; M(xi) is the gray value of the corresponding pixel rate in the filtered image; D(xi) is the Gray value difference; A is the average pixel rate deviation of the entire image.

After calculation, the average pixel rate deviation corresponding to various filtering methods is obtained, as shown in Table 1.

Table 1. Mean pixel rate deviation corresponding to various filtering methods

Filtering method	Additional Noise	Improved smoothing filtering	Median filtering	Mean filtering	Median and mean
Mean pixel rate deviation	14.4957	6.72764	7.17565	7.34539	14.1566
Filtering rate /%	-	53.59	50.50	49.33	2.34

Figure 2 and Table 1 show that the filtering denoising of bridge crack images is very necessary. The improved smoothing filtering algorithm has the most apparent filtering effect on the grayscale images of bridge cracks. The median filtering can effectively protect the edges of the image, the mean filtering makes the bridge cracks blurred, and the filtering method combining the median and the mean has a poor filtering effect and is not suitable for the filtering of bridge crack images.

3. Bridge crack calculation

After processing the bridge crack image, information such as the pixel rate width, pixel rate perimeter, and pixel rate area of the crack can be calculated. The crack pixel rate perimeter can be obtained by counting the distance between adjacent edge points of the crack in the image, and the crack pixel rate area can be calculated by statistical Obtain the pixel rates contained in the edge line of the middle crack, and then obtain the actual perimeter and area of the crack through the pixel rate. The crack width is an essential indicator for bridge detection and evaluation and cannot be directly obtained by counting the statistical pixel rates. This article focuses on the study of the crack width. Calculation (maximum crack width).

Under normal circumstances, the crack direction in the bridge crack image is an irregular curve. The processed bridge crack image is a pixel rate matrix of discrete points in m rows and n columns. The pixel rate width of the crack can be calculated by using the matrix and the relevant characteristics of the crack.

In the crack image pixel rate matrix, the pixel rate coordinates of any point can be expressed in the form (i, Z (i, k)), i=1,2, ..., m; k = 1,2, ..., n. The pixel rate coordinates of the top edge detection point (i.e., the crack edge point) in column k are (i, Z (i, k)), and the pixel rate coordinates of the bottom edge detection point are (j, Z (j, k)). The following equation can be obtained.

Crack vertical pixel rate width P (k):

$$P\ (k) = \ Z\ (i,\ k) - \ Z(\ j,\ k) \tag{8}$$

$Assuming\ M(k) = \frac{z(i,k)+z(j,k)}{2}$,crack inclination $\theta(k)$ can be obtained as follows

$$\theta(k) = \arctan\ arctan\left(\frac{M(k+1)}{2}\right) \tag{9}$$

Pixel rate width W(k) of the crack:

$$W(k) = \ P(k) \times \cos\ cos\ (\theta(k)) \tag{10}$$

The maximum value is taken as the pixel rate width value of the bridge crack.

3.1. Calculation of Actual Crack Width

After the bridge crack pixel rate width Max (w (k)) is determined, the image pixel rate η obtained is calculated to obtain the actual bridge crack width W as follows:

$$W\ =\ \eta\ \times\ Max(w(k)) \tag{11}$$

4. Instance Verification

Based on the above orthopedic video calculation method of concrete bridge cracks, using Visual C ++ 6.0 language programming, using a more reasonable crack image processing algorithm, to achieve bridge crack monitoring based on image technology. This paper takes actual bridge cracks as the test object, 15 bridge images taken by digital cameras were verified, and the crack width measured with a crack observer was compared with the experimental values.

The results suggest that the calculated crack width value is slightly larger than the measured value, and the error value is within 0.05mm. When the crack width is above 0.3mm, the calculated crack width value is very close to the measured width value, and the error is 6 Within the range of 0.2%; when the crack width is between 0.2 ~ 0.3mm, the error is within 10%. When the width of the crack is below 0.2mm, the relative error is greater than 30%, the main reason is that the actual measured crack value is read manually to judge the crack The widest position depends on the experience and feeling of the inspector, it is difficult to determine the widest position of the crack, and the accuracy of the crack observer is 0.1mm, and the crack value calculated by the image is the maximum value of all cracks. It is stipulated in the Prestressed Concrete Bridges and Culverts Design Code (JTGD62-2004) that the full cross-section of the prestressed bridge under the short-term load effect combination and part of the prestressed class A (limited tensile stress) bridge under the long-term load combination Tensile stress is not allowed at the tensile edge, that is, vertical cracks are not allowed, and the maximum crack width allowed for reinforced concrete bridges and partially prestressed Class B (exceeding limit tensile stress) bridges under normal use conditions (class I or II ring The lower non-steel wire or steel strand prestress) is 0.2mm. The " Code for Conservation of Highway Bridge Conservation " (JTGH11-2004) stipulates that vertical cracks in the beam body and longitudinal cracks in the beam body are not allowed for fully prestressed or partially prestressed Class A bridges. The maximum allowable width is 0.2mm, and the maximum permissible width of vertical cracks for reinforced concrete or partially prestressed Class B bridges is 0.25mm, and repair or reinforcement should be performed beyond this value. In summary, the crack identification method proposed in this paper is mainly used for reinforcing steel Crack detection of concrete bridges and Class B prestressed concrete bridges.

5. Conclusion

In this paper, the crack detection technology of concrete bridges based on videos is systematically studied to obtain the following conclusions: 1) The Visual C ++6.0 language is used to develop a program in this paper to compare the relevant algorithms of image processing techniques systematically and obtain the algorithm for bridge crack image processing. Based on instances, it is proved that the proposed bridge crack detection method can be applied to actual detection properly. 2) The pixel rate of bridge crack images is solved by the checkerboard corner calibration method, and the combined algorithm of Harris and SV can identify and calculate the image plane coordinates of corner points accurately to provide technical support for subsequent accurate fracture calculations.

References

[1] Haitao Yuan, Shuai Wang, Jizong Tan. Study on municipal road cracking and surface deformation based on image Recognition [J]. Aip Conference Proceedings, 2017, 1839(1):1- 12.

[2] Dong Liang, Xue-Feng Zhou, Song Wang. Research on Concrete Cracks Recognition based on Dual Convolutional Neural Network [J]. KSCE Journal of Civil Engineering, 2019, 23(10):14-26.

[3] K V Shamshina, V N Migunov, I G Ovchinnikov. Influence of corrosion longitudinal cracks on rigidity and strength of reinforced concrete structures [J]. IOP Conference Series Materials Science and Engineering, 2018, 451(1):20-35.

[4] Hongbo Jiang, Qiang Li, Qisong Jiao. Extraction of Wall Cracks on Earthquake-Damaged Buildings Based on TLS Point Clouds [J]. IEEE Journal of Selected Topics in Applied Earth Observations & Remote Sensing, 2018, 11(9):112-121.

[5] Yang,Jie. Study on the Prediction of the Maximum Crack Extension Location for Surface Cracks [J]. Applied Mechanics & Materials, 2017, 853(6):3-7.

[6] Doo-Yeol Yoo,, Nemkumar Banthia, Young-Soo Yoon. Experimental and numerical study on flexural behavior of ultra-high-performance fiber-reinforced concrete beams with low reinforcement ratios [J]. Canadian Journal of Civil Engineering, 2017, 44(1):18-28.

[7] M. Raniero, M. Calca, D. Fernando, O. Almeida and A. Dal Pai, "Software for automated reading of sunshine duration by Digital Image Processing," in IEEE Latin America Transactions, vol. 18, no. 09, pp. 1599-1605, September 2020, doi: 10.1109/TLA.2020.9381802.

[8] K. Tartarotti Nepomuceno Duarte, M. Andrade Nascimento Moura, P. Sergio Martins and M. A. Garcia de Carvalho, "Brain Extraction in Multiple T1-weighted Magnetic Resonance Imaging slices using Digital Image Processing techniques," in IEEE Latin America Transactions, vol. 20, no. 5, pp. 831-838, May 2022, doi: 10.1109/TLA.2022.9693568.

[9] T. Kutuk-Sert, M. Ozturk, and S. Kutuk, “Digital image processing of warm mix asphalt enriched with nanocolemanite and nanoulexite minerals,” Construction and Building Materials, vol. 399, no. 1, pp. 132542–132550, 2023. doi:10.1016/j.conbuildmat.2023.132542

[10] C. Li, S. Tang, H. K. Kwan, J. Yan and T. Zhou, "Color Correction Based on CFA and Enhancement Based on Retinex With Dense Pixels for Underwater Images," in IEEE Access, vol. 8, pp. 155732-155741, 2020, doi: 10.1109/ACCESS.2020.3019354.

[11] C. He et al., “Correlations between mineral composition and mechanical properties of granite using digital image processing and discrete element method,” International Journal of Mining Science and Technology, vol. 1, no. 1, pp. 1–12, 2023. doi:10.1016/j.ijmst.2023.06.003

[12] Q. Wu, H. Tang, H. Liu and Y. Chen, "Masked Joint Bilateral Filtering via Deep Image Prior for Digital X-Ray Image Denoising," in IEEE Journal of Biomedical and Health Informatics, vol. 26, no. 8, pp. 4008-4019, Aug. 2022, doi: 10.1109/JBHI.2022.3179652.

[13] T. P. Pham Le et al., “Optical coherence tomography and digital image processing for scaling and co-precipitation investigation on reverse osmosis membrane,” Journal of Membrane Science, vol. 677, no. 1, pp. 121658–121666, 2023. doi:10.1016/j.memsci.2023.121658

[14] Z. Fan, J. Lu, C. Wei, H. Huang, X. Cai and X. Chen, "A Hierarchical Image Matting Model for Blood Vessel Segmentation in Fundus Images," in IEEE Transactions on Image Processing, vol. 28, no. 5, pp. 2367-2377, May 2019, doi: 10.1109/TIP.2018.2885495.

[15] B. Lu, B. Bai, and X. Zhao, “Vision-based structural displacement measurement under ambient-light changes via deep learning and Digital Image Processing,” Measurement, vol. 208, no. 1, pp. 112480–112492, 2023. doi:10.1016/j.measurement.2023.112480

[16] Z. Liu, P. Bagnaninchi and Y. Yang, "Impedance-Optical Dual-Modal Cell Culture Imaging With Learning-Based Information Fusion," in IEEE Transactions on Medical Imaging, vol. 41, no. 4, pp. 983-996, April 2022, doi: 10.1109/TMI.2021.3129739.

[17] S. Zeng, C. Zhang, K. Zeng, N. Liang, and S. Song, “Real-time identification of asphalt mixture segregation during paving process using digital imaging technique and four-side static moment,” Construction and Building Materials, vol. 397, no. 1, pp. 132436–132443, 2023. doi:10.1016/j.conbuildmat.2023.132436

[18] M. S. Hosseini, J. A. Z. Brawley-Hayes, Y. Zhang, L. Chan, K. N. Plataniotis and S. Damaskinos, "Focus Quality Assessment of High-Throughput Whole Slide Imaging in Digital Pathology," in IEEE Transactions on Medical Imaging, vol. 39, no. 1, pp. 62-74, Jan. 2020, doi: 10.1109/TMI.2019.2919722.

[19] T. D. Shashikala, S. L. Sunitha, and S. Basavarajappa, “Quantification of worn surface using digital image processing,” Tribology International, vol. 176, no. 1, pp. 107864–107876, 2022. doi:10.1016/j.triboint.2022.107864

[20] P. C. da Silva et al., “Investigation of copper and zinc alloy surface exposed to corrosion environment by Digital Image Processing,” Journal of Materials Research and Technology, vol. 24, no. 1, pp. 9743–9753, 2023. doi:10.1016/j.jmrt.2023.05.174

[21] T. Lukács, C. Pereszlai, G. Magyar, and N. Geier, “Drilling-induced delamination measurement using a novel digital image processing algorithm,” Procedia CIRP, vol. 118, no. 1, pp. 828–832, 2023. doi:10.1016/j.procir.2023.06.142